RSC Advances

ROYAL SOCIETY OF CHEMISTRY

www.rsc.org/advances

Functional effectiveness and diffusion behavior of sodium lactate loaded chitosan/poly (L-lactic acid) film with antimicrobial activity

Hualin Wang[a,c,*], Ru Zhang[a], Junfeng Cheng[a], Huan Liu[a], Linfeng Zhai[a], Shaotong Jiang[b,c]

[a]*School of Chemistry and Chemical Engineering, Hefei University of Technology, Hefei, Anhui 230009, People's Republic of China*

[b]*School of Biotechnology and Food Engineering, Hefei University of Technology, Hefei, Anhui 230009, People's Republic of China*

[c]*Anhui Institute of Agro-Products Intensive Processing Technology, Hefei, Anhui 230009 , People's Republic of China*

Corresponding author: Hualin Wang, hlwang@hfut.edu.cn, Fax: 86-551-62901450, Tel: 86-551-62901450

ABSTRACT: The present work aimed to evaluate the functional effectiveness and diffusion behavior of sodium lactate loaded chitosan/poly (L-lactic acid) (SL-CS/PLLA) film prepared by coating method as a novel active packaging, using Escherichia coli (*E. coli*, 8099) as test bacterium. The hydrogen bonds formed between CS and PLLA improved the thermal stability and caused a decrease in crystalline of the composite film. The incorporation of PLLA increased the hydrophobicity of film and resulted in a decrease in water gain percentage at equilibrium with decreasing CS/PLLA ratio. The PLLA was valid in blocking visible light and invalid in blocking ultraviolet light through films, and the surface color of CS/PLLA films changed distinctively as compared to neat CS film. The decrease of CS/PLLA ratio caused a decrease in both water vapor permeability (WVP) and oxygen permeability (OP), which reached their minimum values at 1.95×10^{-3} g m^{-1} d^{-1} kPa^{-1} and 2.1×10^{-3} cm^2 d^{-1} kPa^{-1} for CS/PLLA ratio at 1:1, respectively. The SL-CS/PLLA film displayed well controlled release and the initial diffusion of SL (M_t/M_∞ <2/3) could be well described by Fickian diffusion equation. The thermodynamic parameters suggested that the diffusion of SL was endothermic and spontaneous, and the increase of temperature and PLLA content in film favored the diffusion of SL.

Keywords: Functional effectiveness; Kinetics; Thermodynamics; Active packaging; Sodium lactate loaded chitosan/poly (L-lactic acid)

1. Introduction

Antibacterial packaging has been widely investigated towards mildly preserved, fresh, tasty and convenient food products with extended shelf-life and controlled quality[1], owing to the efficiency in extending bacterial lag phase, slowing the growth rate of micro-organisms and maintaining food quality and safety during the transport and storage[2, 3]. In particular, biopolymer-based antimicrobial films have been attracting much attention from the food industry with their potential application for a variety of foods[4].

Chitosan (CS) has showed great aptitude for its application in food preservation[5, 6]. Besides its good biodegradation, biocompatibility, nontoxicity and various bio-functionalities, CS also represented interesting properties such as excellent film forming capacity, gas and aroma barrier properties, which made it a suitable material for designing food packaging structures [7]. Since the high sensitivity to moisture and low water barrier properties of neat CS film limited its broader application in antibacterial food packaging, it was required to associate CS with a more moisture-resistant polymer, while maintaining the overall biodegradability of the product [8, 9]. Poly(L-lactic acid) (PLLA), a biodegradable, nontoxic and biocompatible polymer [9-11], has been widely used in drug carriers for a sustained release[12, 13]. PLLA was reported to be of sufficient water resistance [9, 14] and seemed to suit our purpose as a hydrophobic component to modify CS.

A wide variety of antimicrobials have been incorporated into biopolymer-based films for food packaging as antibacterial entities such as nisin[15, 16], bacteriocins[17, 18], lysozyme[19], E-polylysine[20, 21], sorbic acid[22, 23], Na-alginate and κ-carrageenan[24], potassium sorbate and natamycin[25, 26], grape seed extract, malic acid and EDTA[27]. As an important preservative, sodium lactate (SL) have attracted our attention in the present work as antibacterial entity, owing to the ability to control microbial growth, improve sensory attributes and extend the shelf life of various food systems

including beef [28], salmon [29], and fish [30]. Moreover, SL was widely available, economical and generally recognized-as-safe [31]. However, little work has been done on the release of SL from biopolymer-based antimicrobial film. As the antimicrobial activity of film depended on the diffusion of antimicrobial entity, knowledge of diffusivity of the entity is very important in developing an antimicrobial food packaging system[3, 32, 33]. As a supplement, thermodynamic parameters [enthalpy (H^0), entropy (S^0) and Gibbs free energy (G^0)] can also provide some important information regarding the inherent energetic changes associated with the diffusion.

The overall objective of the present study was to evaluate the functional effectiveness and diffusion behavior of sodium lactate loaded chitosan/poly(L-lactic acid) (SL-CS/PLLA) film. The structure and thermal stability, water sorption, color and transparency, water vapor permeability (WVP) and oxygen permeability (OP) of CS/PLLA films as well as the antimicrobial activity of SL-CS/PLLA films were assessed. More attentions were focused on the diffusion of SL from the film by kinetics and thermodynamics towards different CS/PLLA ratios. In the experimental, a representative Gram-negative bacterium Escherichia coli (*E. coli*, 809) was used as test bacterium.

2. Experimental

2.1 Materials

Chitosan (CS, Mw 300 kDa, DD 95%, viscosity 100 m Pa.s) was purchased from Zhejiang Aoxing Biochemical Co., Ltd. (Zhejiang, China). Poly(L-lactic acid) (PLLA, Mw 35 kDa) was prepared in our laboratory. Sodium lactate (SL) was supplied from Sigma (St. Louis, MO, USA). Escherichia coli (*E. coli*, 8099) were provided by China Center of Industrial Culture Collection (Beijing, China). All the other chemical reagents were of analytical grade and available from Sinopharm Chemical Reagent Co. Ltd. (Shanghai, China).

2.2 Sample preparation

CS solution (4 wt%) was prepared by dissolving CS into acetic acid (2.0%, v/v), meanwhile, required PLLA was dissolved into chloroform/ethanol mixture (1:1, v/v) to prepare 10 wt% PLLA solution. The dissolving process was performed at room temperature. Then, serials of CS/PLLA blend solutions with different CS/PLLA ratio (3:1, 2:1, 1:1, 1:2 and 1:3, w/w) were prepared by blending the two polymer solutions. Correspondingly, the films prepared were called CS/PLLA=3/1, CS/PLLA=2/1, CS/PLLA=1/1, CS/PLLA=1/2 and CS/PLLA=1/3, respectively. All the films were preformed on an AFA-III automatic film applicator (Hefei Kejing Material Technology Co., Ltd, China). The homogeneous CS/PLLA blend solution was coated onto a substrate polyethylene (PE) film. After drying at 35 ^{o}C for 72 h, the CS/PLLA films were peeled from the substrate film and vacuum dried at 60 ^{o}C for 24 h in order to remove the residues of chloroform, ethanol, water and acetic acid.

SL-CS/PLLA films were prepared on the AFA-III automatic film applicator and the parameters were the same as that of CS/PLLA films. Required SL (2, 4, 6, 8 and 10%, w/w, based on the weight of CS/PLLA) was added into the CS/PLLA solutions and stirred continuously at room temperature for 4 h before coating on the substrate film.

2.3 Structure and thermal stability

For PLLA powder, neat CS and CS/PLLA=1/1 films, X-ray diffraction (XRD) analysis was measured with a D/max-γB rotating diffractomete (Rigaku, Japan), using CuKa (λ=0.15418 nm). A scan rate of 0.05^{o}/s was applied to record the pattern in the 2θ range of 5-60^{o}. Thermal stability of neat CS and CS/PLLA=1/1 films were assessed using a TGA 209 thermogravimetric analyzer (Netzsch, Germany). The samples were heated from room temperature to 600 ^{o}C at a constant

heating rate of 10 ^{o}C /min under nitrogen flow at rate of 50 ml/min.

2.4 Water sorption test

The hydrophilic or hydrophobic nature of neat CS and CS/PLLA films were evaluated by determining water sorption according to a modified method as described in the articles [34, 35]. Three randomly selected samples (2 cm×2 cm) with of thickness of 100±5 μm from each type of film were first desiccated overnight (containing silica gel), and weighed to determine their dry mass. The weighed films were placed in beakers containing 100 ml of distilled water. Each beaker was covered with parafilm and stored at 25 ^{o}C". The water sorption were evaluated by periodically measuring the weight increment of samples with respect to dry films by a digital balance (accuracy = 0.0001g), after gently bottling the surface with a tissue, until equilibrium was reached. The water gain (WG) was calculated by the following equation:

$$WG(\%) = (m_{Wet} - m_{Dry}) / m_{Dry} \times 100\% \quad (1)$$

where m_{Wet} and m_{Dry} are the weight of wet and dry film, respectively.

2.5 Color and transparency

The surface color of film was measured with a Chroma meter (Konica Minolta, CR-300, Tokyo, Japan). Each film was placed on a white color plate (L=97.63, a=-0.53, b=2.27) as a standard background for measuring color [36, 37] and the parameters [L (lightness), a (red/green) and b (yellow/blue)] were determined by taking an average of six readings from each film. Total color difference (ΔE) was calculated as follows:

$$\Delta E = [(\Delta L)^2 + (\Delta a)^2 + (\Delta b)^2]^{0.5} \quad (2)$$

where ΔL, Δa and Δb are the difference between color value of standard color plate and film.

Optical property of the film was tested by measuring the transparency of films. Each film was

cut into a rectangular block (1 cm ×5 cm in width and length) and directly mounted between two spectrophotometer magnetic cells. Transparency of film was determined by measuring percent transmittance at 280 nm (T_{280}) and 660 nm (T_{660}) using a UV-vis spectrophotometer (754PC, Shanghai Jinghua Technology Instruments Co., Ltd., Shanghai, China).

2.6 Water vapor and oxygen permeability

Water vapor permeability (WVP) data of the film specimens were measured using a modified method as described by Limpan et al[38]. The specimens, sealed on beakers, containing silica gel (0% RH) were placed in incubator containing distilled water. The chamber of incubator was provided with a psychrometer for relative humidity, and the temperature of incubator was maintained at 30 ^{o}C. The moisture absorbed was estimated by weighing the beakers at 3 h intervals during 3 days. WVP (g m^{-1} s^{-1} Pa^{-1}) was determined as follows:

$$WVP = (w \times x)/(A \times t \times \Delta P) \quad (3)$$

where w is the weight gain of beaker (g), x is the film thickness (m), A is the area of exposed film (m^2), t is the time of weight gain (s), and ΔP is the water vapor partial pressure difference (Pa) across the two sides of film calculated on the basis of relative humidity.

Oxygen transmission rate (OTR, according to ASTMD1434) of film was determined at 23 ^{o}C and 0% RH on a N500 gas permeameter (Guangzhou Biaoji packaging equipment Co., Ltd Guangzhou, China). Oxygen permeability (OP) was calculated from OTR (cm^3 m^{-2} d^{-1} kPa^{-1}) as follows:

$$OP = OTR \times thinkness \quad (4)$$

The thickness and open testing area of each sample were approximately 100 μm and 50 cm^2 in three parallel measurements, respectively. Film thickness was measured with a hand-held

136 micrometer (BC Ames Co., Waltham, MA, USA).

137 *2.7 Antibacterial activity assay*

138 *E. coli* bacteria were grown aerobically in Luria-Broth (LB) for 24 h on a shaker platform
139 (SHZ-82, Changzhou Guohua Electric Appliance Co., Ltd., Jiangsu, China) at 200 rpm and 37 ^{o}C.
140 10^8 colony forming units (CFUs) of *E. coli* were monitored by counting the viable cells after
141 appropriate dilution on Nutrient Agar (NA), respectively, which number of per ml was equivalent
142 to 0.1 optical density at 600 nm (OD_{600}), and then it was diluted to 100 ml nutrient broth freshly
143 prepared. Afterwards, the specimen was added to 1ml diluted culture medium at an initial value of
144 OD_{600}. The growth of bacteria was monitored by a spectrophotometer (UV-754PC, Shanghai
145 Jinghua Technology Instruments Co., Ltd., Shanghai, China). The specimen without additional SL
146 was used as a control. The inhibition efficiency of each SL-CS/PLLA film was adopted as *Eq.(5)*

147 $$Inhibition \quad efficiency = [(OD_{600}^{C} - OD_{600}^{S}) / OD_{600}^{C}] \times 100\% \qquad (5)$$

148 where OD_{600}^{C} and OD_{600}^{s} were the OD_{600} values of culture medium for the control and
149 SL-CS/PLLA films at 24 h, respectively. The incubation for each flask was performed on the
150 shaker platform (160 rpm, 37 ^{o}C) and the experiment was repeated three times for each contents.

151 *2.8 Diffusion test*

152 Films were cut into squares (5 cm×5 cm) and the film thickness was measured with the
153 hand-held micrometer. Afterwards, the film was covered with aluminum foil tape on one side and
154 immersed in an Erlenmeyer flask containing 100 ml distilled water. The flaks were shaken
155 continuously on the shaker platform (100 rpm, 25^{o}C) and achieved diffusion equilibration. The
156 absorbance at 206 nm was measured with the spectrophotometer to determine the concentrations
157 of SL diffused in the solution at different time and diffusion equilibration.

158 The cumulative release percentages of SL from films were calculated as following:

159 $$Cumulative \quad release = (M_t / M_0) \times 100\% \qquad (6)$$

160 where M_t (μg) is the SL diffused at time t, M_0 (μg) is the total trapped or entrapped SL.

161 The pH values of diffusion solutions were adjusted to be at pH 6.5±0.1 by adding a thimbleful
162 of 0.01 M HCl or 0.01 M NaOH solution. According to our experimental data, a pH approximately
163 6.5 was representative.

164 *2.9 Statistical analysis*

165 Each experiment was repeated three times. Statistical analysis was performed using the
166 unpaired Student's t-test, and the results were expressed as the means ± standard deviation (SD). A
167 value of $p < 0.05$ was considered to be statistically significant.

168 **3. Results and discussion**

169 *3.1 Structure and thermal stability*

170 The interactions between CS and PLLA in CS/PLLA films have been confirmed to be
171 intermolecular hydrogen bonds from FTIR by our previous work[16], and the structure scheme was
172 proposed as shown in Fig. 1A. Similar scheme was presented by Chen et al[39]. In order to
173 investigate the crystalline of CS/PLLA film, XRD measurements were performed towards PLLA
174 powder, CS film and representative CS/PLLA=1/1 film. As could be seen from Figure 1B,
175 main peaks of PLLA at 2θ = 15.1, 17.0, 19.3 and 22.5° indicated the crystalline structure of
176 PLLA[40, 41], meanwhile, peaks of CS film around 2θ=8.3, 11.2 and 18.1° were corresponded to an
177 amorphous structure of CS[4, 42, 43]. In the XRD profile of CSP/PLLA film, the characteristic peaks
178 of PLLA were not observed, at the same time, peaks around 2θ = 11.2 and 18.1° for CS film were
179 sharply weakened and that around 2θ=8.3 disappeared. This is likely to be that the intermolecular

hydrogen bonds formed among PLLA carbonyls and CS amino groups (Fig. 1A) suppressed the crystallization of film matrix[44].

TGA were performed to evaluate the thermal stability of CS/PLLA film with respect to CS film. The TGA curves were similar in shape and composed of three distinguishing weight loss stages (Fig.2.). For CS film, weight loss 8.4% between 40-246 ^{o}C was mainly corresponded to the evaporation of absorbed and bound water, the residue of chloroform, ethanol and acetic acid as well[8, 45-48], weight loss 71.6% between 246-319 ^{o}C was associated with the chemical dehydration of the inner molecule due to hydroxyl condensation and cleavage of C–O and C–C linkages, weight loss 19.5% between 430-530 ^{o}C was probably due to the cleavages of O–N and O–O linkages, and beyond 530 ^{o}C only the residue char remained. CS/PLLA film exhibited better thermal stability as compared to CS film, weight loss 10.69% at 40-315 ^{o}C, weight loss 62.4% at 315-361 ^{o}C, weight loss 21.3% at 437-566 ^{o}C and beyond 566 ^{o}C more residues remained owing to the incorporation of PLLA. The TGA data showed that the initial decomposition temperature for CS/PLLA films was higher than that for CS films by 69 ^{o}C in degree. The reason was that the strong interaction of hydrogen bonds formed between CS and PLLA delayed the decomposition process.

3.2 Water sorption

Water sorption was an important factor for predicting the stability and quality changes of food product during packaging and storage[34, 49]. The water sorption profiles for films were illustrated in Fig.3A. As could be seen from this figure, all the curves showed a rapid water sorption in the first few minutes. The CS/PLLA=1/3 film absorbed almost 500 % water for 15min while in the case of the neat CS film the uptake content could go up to 3000% of weight gain,

after then, the two samples could not be weighted due to dissolution and degradation of the film matrix. It is noteworthy that the incorporation of PLLA increased the hydrophobicity of film and caused a decrease in water gain percentage at equilibrium with decreasing CS/PLLA ratio. The digital photograph of each film absorbing water for 15 min was shown in Fig.3B. Corresponding to water gain curves, the neat CS [Fig.3B (a)] and CS/PLLA=1/3 [Fig.3B (f)] films displayed an easily dissolvable and biodegradable appearance, while the rest films became increasingly curly [Fig.3B (b-e)] associated with the enhancement of hydrophobicity caused by the increase of PLLA.

3.3 Color and transparency

Surface color was an important parameter of food packaging films since it was closely related to the general appearance and consumer acceptance [34, 50, 51]. Surface color parameters of films were summarized in Table 1. Apparently, neat CS film was transparent with deep greenish yellow tint, which was indicated by higher lightness (higher Hunter L) value, lower green (lower Hunter a) value, higher yellowness (higher Hunter b) value, and consequently higher total color difference value (ΔE). The ΔE value of neat CS film was 11.25, which was in good agreement with the reported value of 11.2 [4]. Moreover, the CS/PLLA films (except CS/PLLA=1/3) were less transparent with slight yellowish tint. The L-values decreased slightly and a-values decreased significantly ($p<0.05$), while b-values increased significantly ($p<0.05$) by the incorporation of PLLA into CS matrix. Therefore, the values of ΔE calculated by *Eq.(2)* increased profoundly ($p<0.05$). The transmission of ultraviolet and visible light was very important to preserve and protect products until they reach the consumer as well as to get an attractive transparent package. Consequently, it was necessary to determine the influence of the neat CS and CS/PLLA films on

the UV and visible transmission (Table 1). It was interesting to note that T_{280} values for the CS/PLLA films (except CS/PLLA=1/3) were decreased slightly ($p>0.05$) as compared to neat CS film, but T_{660} values were decreased profoundly ($p<0.05$). This result indicated that the PLLA was valid in blocking visible light and invalid in blocking ultraviolet light through the films. Whereas, the result data of CS/PLLA=1/3 film was distinctively different from the other CS/PLLA films in surface color and transparency, which was mainly attributed to phase separation between CS and PLLA[16].

3.4 Water vapor and oxygen permeability

Water vapor permeability (WVP) is defined as the ease of moisture for penetrating and passing through a material[52]. As it could be seen from Fig.4A, the WVP of films decreased with the decrease of CS/PLLA ratio and reached the minimum value 1.95×10^{-3} g m^{-1} d^{-1} kPa^{-1} for CS/PLLA=1/1. The reasons may be attributed to the high crosslink effects from the intermolecular hydrogen bonds between CS and PLLA molecules, which makes the structure of film become more compact[53]. Subsequently, the WVP of films increased once more (from CS/PLLA=1/1 to CS/PLLA=1/2) owing to the higher hydrophobicity of PLLA as compared to CS. Nevertheless, the WVP of CS/PLLA=1/3 was slightly lower than that of CS/PLLA=1/2 film owing to the phase separation.

Oxygen permeability (OP) of food packaging is generally considered since it is related to the development of off-flavors, off-odors and nutritional loss associated with oxidation in foodstuffs [54]. As could be seen from Fig.4A, the OP of films significantly decreased with the decrease of CS/PLLA ratio and reached the minimum value 2.1×10^{-3} cm^2 d^{-1} kPa^{-1} for CS/PLLA=1/1, and then increased seriously again. The reason was also associated with crosslink effects formed by

intermolecular hydrogen bonds between CS and PLLA molecules. Based on WVP and OP results, an appropriate CS/PLLA ratio at 1:1 and above was used to prepare SL-CS/PLLA antimicrobial films.

3.5 Antimicrobial activity evaluation

Fig.4B depicted the effects of SL contents on inhibition efficiency of SL-CS/PLLA films towards *E. coli* after incubation at 37 ^{o}C for 24 h. It was found that the inhibition efficiency of the films increased sharply with SL contents below 6%, and then increased slightly before reached a plateau. The releasing dosage of SL into bacterial suspension increased in quantity with an increase of the SL content in SL-CS/PLLA films, hence the growth of *E. coli* was inhibited effectively and the inhibition efficiency increased correspondingly. While SL content reached 6%, the inhibition efficiency was beyond 95%, after then, the increase of SL content had no slight effect on the enhancement of antimicrobial activity against *E. coli*.

3.6 Diffusion kinetics

3.6.1 Release of SL

According to WVP and OP results, the cumulative release percentages of SL from SL-CS/PLLA films (CS/PLLA ratios at 3:1, 2:1 and 1:1) were calculated according to *Eq.(6)* and plotted versus time as shown in Fig. 5A. Each release curve showed a similar initial burst release phenomenon, and reached a plateau after a significantly increase in cumulative release percentage, suggesting a good controlled release behavior for SL-CS/PLLA film[55]. In addition, the cumulative release percentage at diffusion equilibrium increased with decreasing CS/PLLA ratio. The initial burst release was attributed to the diffusion of SL on or near the surface of film under the diffusion driving force by SL content [25, 56, 57]. Afterwards, a gradual increase in the cumulative release was

268 associated with the diffusion of SL being trapped into the inner core of the matrix, which would
269 take longer time to be released owing to the longer diffusion pathway. PLLA is linear hydrophobic
270 aliphatic polyester, while CS is a linear hydrophilic polysaccharide. SL had the better affinity
271 towards CS as compared to PLLA owing to stronger electrostatic interaction between the positive
272 charged CS at low acidic medium and negative charged lactate ions from hydrolyzed SL.
273 Therefore, the cumulative percentage of SL at equilibrium increased with the decrease of CS/PVA
274 ratio.

275 *3.6.2 Estimation of diffusivity of SL*

276 On the basis of Fig. 5A, M_t/M_∞ of the amount of SL diffused at time t (M_t) and at equilibrium
277 (M_∞) was calculated and plotted as a function of time (Fig. 5B). The diffusion coefficients (D)
278 were calculated from the following solutions [25, 32, 58, 59] of from Fick's second law [58] assuming that
279 the dispersion of SL in film was uniform and the concentration of SL in the aqueous medium was
280 zero; the diffusion of SL was regarded as one-dimensional diffusion (As mentioned in
281 experimental, the specimen was covered with aluminum foil tape on one side) and a non-steady
282 state phenomenon of non-concentration-dependent diffusion [32].

283 $$\frac{M_t}{M_\infty} = 1 - \sum_{n=0}^{\infty} \frac{8}{(2n+1)^2 \pi^2} exp\left\{ - \frac{D(2n+1)^2 \pi^2 t}{h^2} \right\} \quad (7)$$

284 where h (m) is the thickness of SL-CS/PLLA film measured with the hand-held micrometer. In
285 cases where M_t/M_∞ <2/3 the following equation was applied [25, 58-60]:

286 $$\frac{M_t}{M_\infty} = 4\left(\frac{Dt}{\pi h^2} \right)^{\frac{1}{2}} = kt^{\frac{1}{2}} \quad (8)$$

287 where k ($1/s^{1/2}$) is slope of the linear regression of M_t/M_∞ versus $t^{1/2}$. Consequently, the diffusivity
288 could be counted by the following equation [32]:

$$D = \left(\frac{kh}{4}\right)^2 \pi \quad (9)$$

As could be seen from Fig. 5B, M_t/M_∞ depended on film composition and decreased with increasing CS/PLLA ratio at given time owing to the better affinity of SL towards CS as compared to PLLA. Moreover, a similar shape was presented in each curve by increasing sharply before reaching a plateau. The inset of Fig. 5B showed a strong linearity with respect to $t^{1/2}$ predicted by *Eq. (8)* for the initial portion of the curve (M_t/M_∞ <2/3), correspondingly, the D value of each film was calculated by *Eq. (9)* and listed in Table 2. Similarly, the D values at 5 and 45°C were obtained and summarized in Table 2. The higher correlation coefficient (R^2>0.998) indicated that that Fickian diffusion was valid to described the initial diffusion (M_t/M_∞ <2/3) of SL. As expected, the higher affinity of SL towards CS resulted in an increase in D value with decreasing CS/PLLA ratio at each given temperature, and a higher temperature caused an increase in D value for the same film.

Temperature dependence of diffusion coefficient (D) is described by the logarithmic transform of Arrhenius activation energy equation [32, 56, 61].

$$ln\ D = ln\ D_0 - \frac{E_a}{RT} \quad (10)$$

where D_0 (m^2/s) is a constant, E_a (J/mol) is activation energy of the diffusivity of SL, R (J/mol K) is universal gas constant and T (K) is absolute temperature. The Arrhenius plots (Fig. 6A) were derived from the equation of *Eq*. (10) based on Table 2, which allowed us to calculate the corresponding E_a in Table 3. The high correlation coefficient values (R^2 > 0.999) for each film indicated that Arrhenius activation model was valid to describe the temperature dependence of D for SL. The decreasing CS/PLLA ratio resulted in a decrease in E_a values, suggesting the less sensitive of diffusivity towards temperature change[32]. In addition, the lower E_a value predicted a

311 weaker interaction between SL and CS/PLLA matrix, since less work in the form of energy was
312 needed to overcome the energetic barrier [62]. As mentioned previously, SL had better affinity
313 towards CS as compared to PLLA. Hence, the decrease of CS/PLLA ratio resulted in a decrease in
314 *Ea* value at same temperature.

315 *3.7 Diffusion thermodynamics*

316 A distribution coefficient (K_d) associated with the total entrapped SL (M_0) in film and the
317 amount of SL diffused at equilibrium (M_∞) was adapted:

318 $$K_d = \frac{M_\infty}{M_0 - M_\infty} \cdot \frac{m}{V} \quad (11)$$

319 where V (ml) was the volume of solution and m(g) was the weight of each specimen. The enthalpy
320 change (ΔH^0) and entropy change (ΔS^0) for the diffusion of SL from film were calculated by the
321 slope and intercept of the plot of lnK_d *versus* 1/T (Fig. 6B) based on temperature-dependent
322 distribution coefficient equation:

323 $$\ln K_d = \frac{\Delta S^0}{R} - \frac{\Delta H^0}{RT} \quad (12)$$

324 where R (8.314 J·mol^{-1}·K^{-1}) was the ideal gas constant, and T (K) was the temperature in Kelvin.
325 Meanwhile, the corresponding Gibbs free energy (ΔG^0) was calculated by a general expression:

326 $$\Delta G^0 = \Delta H^0 - T\Delta S^0 \quad (13)$$

327 The calculated diffusion thermodynamic parameters were listed in Table 4. The positive ΔH^0
328 suggested the endothermic diffusion, because kinetic energy was needed for the diffusion of
329 entrapped SL through CS/PLLA matrix. The positive ΔS^0 might be associated with the affinity and
330 dispersion change of SL in the films. Noteworthily, the value of ΔG^o was negative and decreased
331 with increasing temperature, indicating that the diffusion of SL in CS/PLLA matrix was
332 spontaneous and the spontaneity was improved by increasing temperature. Moreover, the decrease

in CS/PLLA ratio caused a decrease in ΔG^o values. This information confirmed that the increase of PLLA in film favored the diffusion of SL owing to the lower affinity towards PLLA as compared to CS.

4. Conclusions

The diffusion behavior and functional effectiveness were evaluated towards a novel SL-CS/PLLA antibacterial film. The strong interaction of hydrogen bonds formed between CS and PLLA improved the thermal stability and caused a decrease in crystalline of the composite film. The incorporation of PLLA increased the hydrophobicity of film and resulted in a decrease in water gain percentage at equilibrium with decreasing CS/PLLA ratio. The PLLA was valid in blocking visible light and invalid in blocking ultraviolet light through the films, and the surface color of CS/PLLA films changed distinctively as compared to neat CS film. The decrease of CS/PLLA ratio caused a decrease in both WVP and OP, which reached their minimum values for CS/PLLA ratio at 1:1, respectively. The SL-CS/PLLA film displayed well controlled release of SL and the initial diffusion of SL (M_t/M_∞ <2/3) from film could be well described by Fickian diffusion equation. The thermodynamic parameters suggested that the diffusion of SL was endothermic and spontaneous, and the increase temperature and PLLA in film favored the diffusion of SL. These results suggested a potential application as a new active film in controlled release and antimicrobial activity against *E. coli* towards food packaging.

Acknowledgments

Financial support from National Natural Science Foundation of China (31371859) is gratefully acknowledged.

References

1. M. Aider, *LWT-Food Sci. Technol.*, 2010, **43**, 837-842.
2. G. Mauriello, E. De Luca, A. La Storia, F. Villani and D. Ercolini, *Lett. Appl. Microbiol.*, 2005, **41**, 464-469.
3. S. Min, T. R. Rumsey and J. M. Krochta, *J. Food Eng.*, 2008, **84**, 39-47.
4. J.-W. Rhim, S.-I. Hong, H.-M. Park and P. K. Ng, *J. Agr. Food Chem.*, 2006, **54**, 5814-5822.
5. M. D. R. Moreira, M. Pereda, N. E. Marcovich and S. I. Roura, *J. Food Sci.*, 2011, **76**, M54-M63.
6. P. Dutta, S. Tripathi, G. Mehrotra and J. Dutta, *Food Chem.*, 2009, **114**, 1173-1182.
7. C. Caner, *J. Sci. Food Agr.*, 2005, **85**, 1897-1902.
8. J. Bonilla, E. Fortunati, M. Vargas, A. Chiralt and J. Kenny, *J. Food Eng.*, 2013, **119**, 236-243.
9. N. E. Suyatma, A. Copinet, L. Tighzert and V. Coma, *J. Polym. Environ.*, 2004, **12**, 1-6.
10. C.-C. Chen, J.-Y. Chueh, H. Tseng, H.-M. Huang and S.-Y. Lee, *Biomaterials*, 2003, **24**, 1167-1173.
11. J. Dutta and P. Dutta, *Everymans Sci. vol. XLI.*, 2006, **2**: 85-103.
12. J. Dutta, V.S. Tripathi and P.K. Dutta, *Asian Chitin J.*, 2010, **6**, 29-34.
13. J. Dutta, V. Tripathi, M. Chattopadhyaya and P. Dutta, *Asian Chitin J.*, 2005, **1**, 79-86.
14. O. Martin, E. Schwach and Y. Couturier, *Starch - Stärke*, 2001, **53**, 372-380.
15. T. Jin and H. Zhang, *J.f Food Sci.*, 2008, **73**, M127-M134.
16. H. Wang, H. Liu, C. Chu, Y. She, S. Jiang, L. Zhai, S. Jiang and X. Li, *Food Bioproc. Tech.*, 2015, **8**, 1657-1667.
17. J. Cleveland, T. J. Montville, I. F. Nes and M. L. Chikindas, *Int. J.Food Microbiol.*, 2001, **71**, 1-20.
18. L. H. Deegan, P. D. Cotter, C. Hill and P. Ross, *Int. Dair. J.*, 2006, **16**, 1058-1071.
19. S. Min, L. J. Harris, J. H. Han and J. M. Krochta, *J. Food Protect.*, 2005, **68**, 2317-2325.
20. T. Yoshida and T. Nagasawa, *Appl. Microbiol.Biot.*, 2003, **62**, 21-26.
21. L. Shih, M.-H. Shen and Y.-T. Van, *Bioresource Technol.*, 2006, **97**, 1148-1159.
22. A. Giannakopoulos and S. Guilbert, *Int. J. Food Sci. Tec.*, 1986, **21**, 477-485.
23. A. Redl, N. Gontard and S. Guilbert, *J. Food Sci.*, 1996, **61**, 116-120.
24. D. S. Cha, J. H. Choi, M. S. Chinnan and H. J. Park, *LWT-Food Sci. Technol.*, 2002, **35**, 715-719.
25. M. Moditsi, A. Lazaridou, T. Moschakis and C. G. Biliaderis, *Food Hydrocolloid.*, 2014, **39**, 195-203.
26. G. Mitrakas, K. Koutsoumanis and H. Lazarides, *Innov. Food Sci. Emerg.*, 2008, **9**, 550-555.
27. V. Gadang, N. Hettiarachchy, M. Johnson and C. Owens, *J. Food Sci.*, 2008, **73**, M389-M394.
28. K. I. Sallam and K. Samejima, *LWT-Food Sci. Technol.* 2004, **37**, 865-871.
29. A. Nykänen, K. Weckman and A. Lapveteläinen, *Int. J. Food Microbiol.*, 2000, **61**, 63-72.
30. G. Boskou and J. Debevere, *Food Addit. Contam.*, 2000, **17**, 17-25.
31. K. I. Sallam, *Food control*, 2007, **18**, 566-575.
32. J. Choi, W. Choi, D. Cha, M. Chinnan, H. Park, D. Lee and J. Park, *LWT-Food Sci. Technol.*, 2005, **38**, 417-423.
33. T. H. Varzakas, G. C. Leach, C. J. Israilides and D. Arapoglou, *Enzym. Microb. Tech.*, 2005, **37**, 29-41.
34. M. Abdollahi, M. Rezaei and G. Farzi, *J. Food Eng.*, 2012, **111**, 343-350.
35. M. Lavorgna, F. Piscitelli, P. Mangiacapra and G. G. Buonocore, *Carbohydr. Polym.*, 2010, **82**,

291-298.
36. S. Shankar, X. Teng, G. Li and J.-W. Rhim, *Food Hydrocolloid.*, 2015, **45**, 264-271.
37. J.-W. Rhim and L.-F. Wang, *Carbohydr. Polym.*, 2013, **96**, 71-81.
38. N. Limpan, T. Prodpran, S. Benjakul and S. Prasarpran, *J. Food Eng.*, 2010, **100**, 85-92.
39. C. Chen, L. Dong and M. K. Cheung, *Eur. Polym. J.*, 2005, **41**, 958-966.
40. H. Tsuji and H. Muramatsu, *J. Appli. Polym. Sci.*, 2001, **81**, 2151-2160.
41. H. Yuan, X. Qiao and J. Ren, *J. Macromol. Sci. A*, 2008, **45**, 754-760.
42. K. Ogawa, S. Hirano, T. Miyanishi, T. Yui and T. Watanabe, *Macromolecules*, 1984, **17**, 973-975.
43. S.-F. Wang, L. Shen, W.-D. Zhang and Y.-J. Tong, *Biomacromolecules*, 2005, **6**, 3067-3072.
44. G. Li, Y. Zhuang, Q. Mu, M. Wang and Y. e. Fang, *Carbohyd. Polym.*, 2008, **72**, 60-66.
45. A. T. Paulino, J. I. Simionato, J. C. Garcia and J. Nozaki, *Carbohyd. Polym.*, 2006, **64**, 98-103.
46. C.-H. Chen, F.-Y. Wang, C.-F. Mao, W.-T. Liao and C.-D. Hsieh, *Int. J. Biol. Macromol.*, 2008, **43**, 37-42.
47. K. Lewandowska, *Thermochim. Acta*, 2009, **493**, 42-48.
48. S. Tripathi, G. Mehrotra and P. Dutta, *Int. J. Biol. Macromol.,* 2009, **45**, 372-376.
49. P. Srinivasa, M. Ramesh and R. Tharanathan, *Food hydrocolloid.*, 2007, **21**, 1113-1122.
50. P. Srinivasa, M. Ramesh, K. Kumar and R. Tharanathan, *Carbohyd. Polym.*, 2003, **53**, 431-438.
51. P. Kanmani and J.-W. Rhim, *Carbohyd. Polym.*, 2014, **106**, 190-199.
52. I. M. Jipa, M. Stroescu, A. Stoica-Guzun, T. Dobre, S. Jinga and T. Zaharescu, *Nucl. Instrum. Methods Phys. Res., Sect. B*, 2012, **278**, 82-87.
53. S. M. Ojagh, M. Rezaei, S. H. Razavi and S. M. H. Hosseini, *Food Chem.*, 2010, **122**, 161-166.
54. M. Fabra, A. Hambleton, P. Talens, F. Debeaufort and A. Chiralt, *Food Hydrocolloid*, 2011, **25**, 1441-1447.
55. N. C. S. Selvam, A. Manikandan, L. J. Kennedy and J. J. Vijaya, *J. Colloid Interf. Sci.*, 2013, **389**, 91-98.
56. B. Ouattara, R. Simard, G. Piette, A. Begin and R. Holley, *J. Food Sci.*, 2000, **65**, 768-773.
57. M. Ozdemir and J. Floros, *J. Food Eng.*, 2001, **47**, 149-155.
58. J. Crank, *The mathematics of diffusion*, Clarendon press Oxford, 1975.
59. C. M. Yoshida, C. E. N. Bastos and T. T. Franco, *LWT-Food Sci. Technol.*, 2010, **43**, 584-589.
60. I. Malley, J. Bardon, M. Rollet, J. Taverdet and J. Vergnaud, *Drug Dev. Ind. Pharm.*, 1987, **13**, 67-79.
61. J. H. Han and J. D. FLOROS, *J. Food Process. Preserv.*, 1998, **22**, 107-122.
62. M. Chen, Z. W. Wang, C. Y. Hu and J. L. Wang, *Packag. Technol. Sci.*, 2012, **25**, 485-492.

Table and figure captions

Table captions

Table 1 Color and transparency of neat CS and CS/PLLA composite films.

Table 2 Diffusivity of SL films with different CS/PLLA ratios (T=298.15 K, pH=6.5 ± 0.1, SL 6 wt %)

Table 3 Activation energy of SL from films with different CS/PLLA ratios (pH=6.5 ± 0.1, SL 6 wt %)

Table 4 Thermodynamic parameters for SL from films with different CS/PLLA ratios (pH=6.5 ± 0.1, SL 6 wt%)

Figure captions

Fig. 1. (A) Proposed structure of CS/PLLA.; **(B)** XRD profiles of PLLA powder, CS film and CS/PLLA=1/1 film.

Fig. 2. TGA curves of neat CS and CS/PLLA=1/1 films.

Fig. 3. (**A**)Water sorption profiles of neat CS and CS/PLLA films (25℃, pH=7). The data (mean± SD) are results from three independent experiments; (B) Digital photographs of films absorbing water for 15 min: (a) represented neat CS film, (b-f) represented CS/PLLA=3/1, 2/1, 1/1, 1/2 and 1/3, respectively.

Fig. 4. (A) Effects of CS/PLLA ratios on WVP and OP and (B) Effects of SL content on inhibition efficiency of the films against *E. coli* (CS/PLLA=1:1, propagated 24 h, 37 ^{o}C). The data (mean± SD) are results from three independent experiments.

Fig. 5. (A) The cumulative release of SL from films (T=25 ^{o}C, pH=6.5 ± 0.1, SL 6 wt %); (B) M_t/M_∞ versus time, inset: linear regression of M_t/M_∞ versus square root of time (T=25 ^{o}C, pH=6.5 ± 0.1, SL 6 wt%). The data (mean±SD) are results from three independent experiments..

Fig. 6. (A) Effects of temperature on diffusion coefficient (CS/PLLA=1:1, pH=6.5 ± 0.1, SL 6 wt%) and (B) Liner plots of lnK_d versus *1/T* for CS/PLLA films (pH=6.5 ± 0.1, SL 6 wt%). The data (mean±SD) are results from three independent experiments.

Table 1 Color and transparency of neat CS and CS/PLLA composite films.

Films	L	a	b	Δ E	T_{280nm} (%)	T_{660nm} (%)
Neat CS	93.6 ± 0.10^{d}	-2.6 ± 0.13^{a}	12.5 ± 0.14^{d}	11.25 ± 0.12^{c}	93.20 ± 0.51^{b}	84.53 ± 1.78^{a}
3:1	97.6 ± 0.32^{c}	-0.56 ± 0.26^{ab}	2.33 ± 0.06^{c}	0.09 ± 0.00^{a}	85.40 ± 0.72^{e}	9.32 ± 0.43^{c}
2:1	96.74 ± 0.2^{a}	-0.85 ± 0.27^{ab}	3.04 ± 0.15^{d}	1.22 ± 0.04^{b}	81.73 ± 1.43^{f}	9.02 ± 0.34^{d}
1:1	96.47 ± 0.2^{a}	-1.66 ± 0.52^{ac}	4.92 ± 0.16^{ad}	3.10 ± 0.15^{ab}	81.70 ± 2.01^{d}	8.80 ± 0.45^{f}
1:2	94.0 ± 0.15^{a}	-2.20 ± 0.03^{b}	7.15 ± 0.08^{b}	6.29 ± 0.23^{ad}	81.00 ± 1.26^{c}	4.27 ± 0.08^{b}
1:3	97.4 ± 0.52^{b}	0.52 ± 0.22^{c}	-2.35 ± 0.11^{a}	4.74 ± 0.14^{d}	84.63 ± 2.07^{a}	20.80 ± 0.13^{e}

Data with the same superscript letter in the same column indicate that they are not statistically different ($p > 0.05$). The data (mean ± SD) are results from six independent experiments.

Table2 Diffusivity of SL films with different CS/PLLA ratios (T=298.15 K, pH=6.5 ± 0.1, SL 6 wt %)

CS/PLLA ratio	Temperature (°C)	$D(\times10^{-14}m^2/s)$ [a]	R^2 [b]
3:1	5	3.33 ± 0.043	0.99852
	25	18.01 ± 0.50	0.99986
	45	81.47 ± 2.04	0.99923
2:1	5	5.58 ± 0.28	0.99878
	25	25.51 ± 1.05	0.99976
	45	93.03 ± 2.88	0.99925
1:1	5	7.66 ± 0.22	0.99868
	25	30.03 ± 1.06	0.99984
	45	102.23 ± 2.28	0.99857

[a]D was calculated using *Eq.(9)*. The data (mean ± SD) are results from three independent experiments. [b]Given correlation coefficient (R^2) was the largest one among replications (n=3).

Table 3 Activation energy of SL from films with different CS/PLLA ratios (pH=6.5 ± 0.1, SL 6 wt %

CS/PLLA ratio	E_a (kJ/mol) [a]	R^{2} [b]
3:1	57.76±2.03	0.99982
2:1	50.85±1.18	0.99986
1:1	46.79±1.92	0.99956

[a]*Ea* was calculated using *Eq.(10)*. The data (mean±SD) are results from three independent experiments. [b]Given correlation coefficient (R^2) was the largest one among replications (n=3)

Table 4 Thermodynamic parameters for SL from films with different CS/PLLA ratios (pH=6.5 ± 0.1, SL 6 wt%)

CS/PLLA ratio	ΔH^0 (kJ/mol) [a]	ΔS^0 (J/(mol·K)) [a]	ΔG^0 (kJ/mol) [b]		
			278.15K	298.15K	318.15K
3:1	16.36±0.40	68.64±1.92	-2.7±0.14	-4.1±0.05	-5.48±0.19
2:1	16.10±0.21	72.32±1.30	-4.02±0.17	-5.46±0.23	-6.91±0.16
1:1	14.69±0.31	72.97±1.53	-5.61±0.15	-7.07±0.17	-8.53±0.14

[a]ΔS^0 and ΔH^0 were calculated using *Eq.(12)*. [b]ΔG^0 were calculated using *Eq.(13)*. The data (mean ±SD) are results from three independent experiments

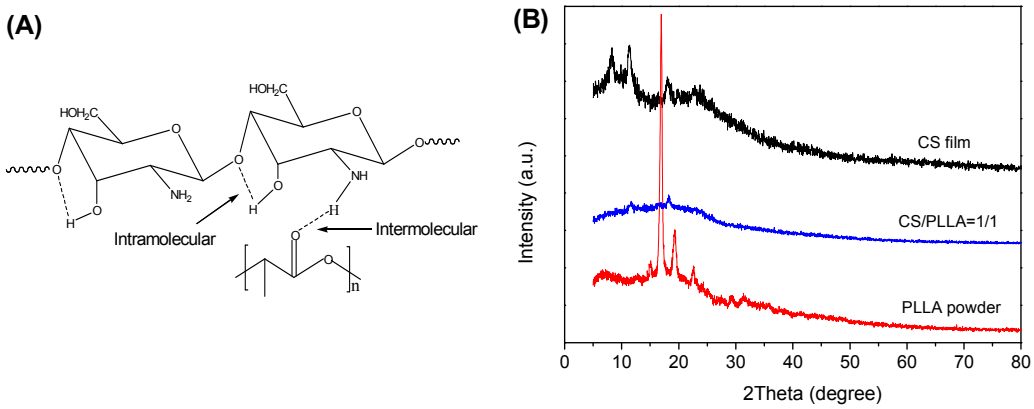

Fig. 1. (A) Proposed structure of CS/PLLA.; **(B)** XRD profiles of PLLA powder, CS film and CS/PLLA=1/1 film.

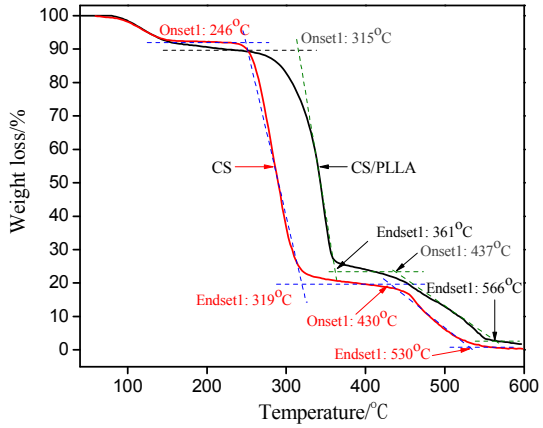

Fig. 2. TGA curves of neat CS and CS/PLLA=1/1 films.

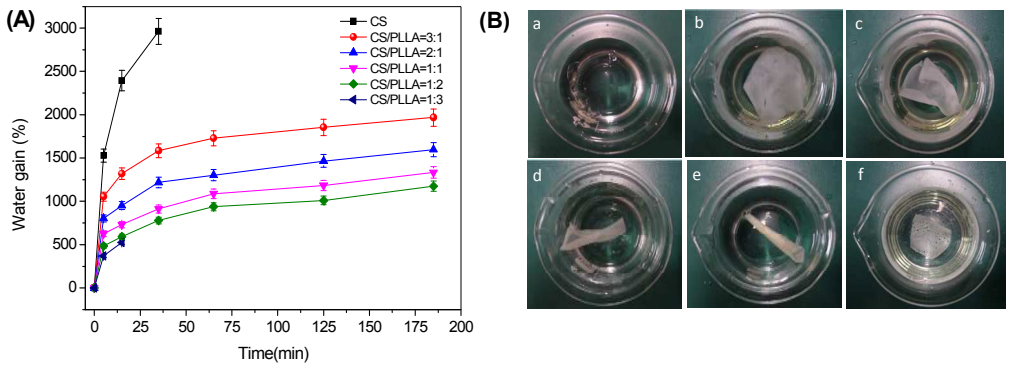

Fig. 3. (**A**)Water sorption profiles of neat CS and CS/PLLA films (25℃, pH=7). The data (mean ± SD) are results from three independent experiments; (B) Digital photographs of films absorbing water for 15 min: (a) represented neat CS film, (b-f) represented CS/PLLA=3/1, 2/1, 1/1, 1/2 and 1/3, respectively.

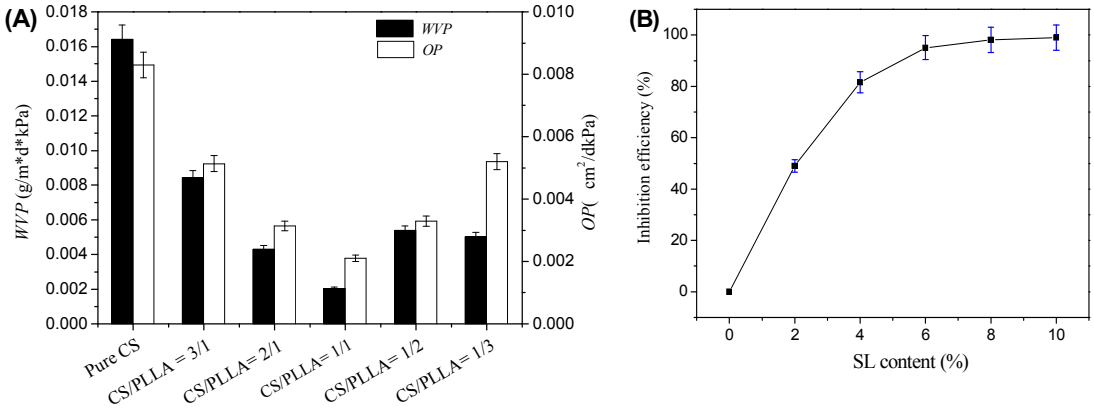

Fig. 4. (A) Effects of CS/PLLA ratios on WVP and OP and (B) Effects of SL content on inhibition efficiency of the films against *E. coli* (CS/PLLA=1:1, propagated 24 h, 37 ^{o}C). The data (mean ± SD) are results from three independent experiments.

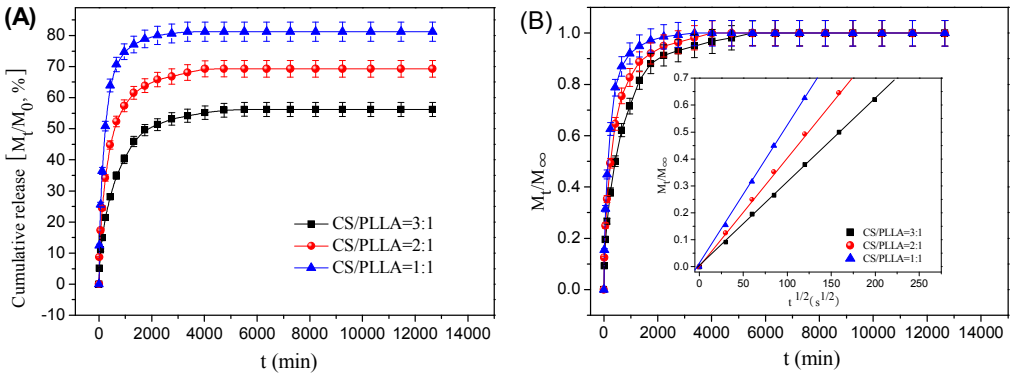

Fig. 5. (A) The cumulative release of SL from films (T=25 ^{o}C, pH=6.5 ± 0.1, SL 6 wt %); (B) M_t/M_∞ versus time, inset: linear regression of M_t/M_∞ versus square root of time (T=25 ^{o}C, pH=6.5 ± 0.1, SL 6 wt%). The data (mean ± SD) are results from three independent experiments..

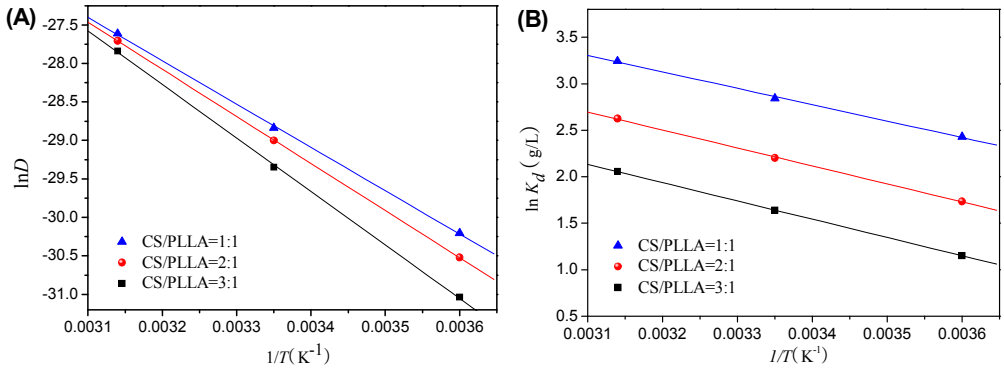

Fig. 6. (A) Effects of temperature on diffusion coefficient (CS/PLLA=1:1, pH=6.5 ± 0.1, SL 6 wt%) and (B) Liner plots of lnK_d versus *1/T* for CS/PLLA films (pH=6.5 ± 0.1, SL 6 wt%). The data (mean±SD) are results from three independent experiments.

Table of contents entry

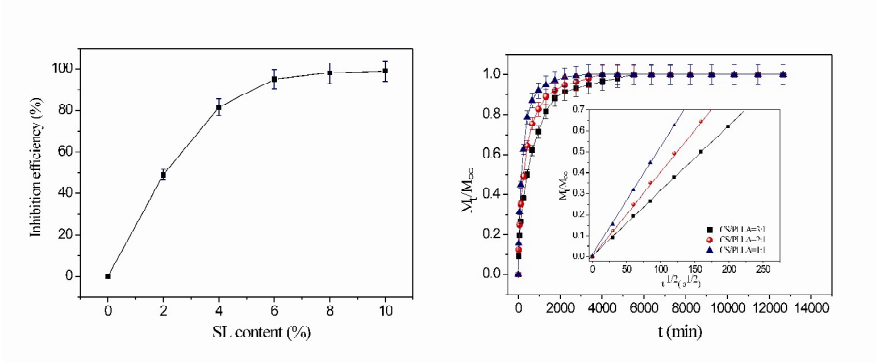

Functional effectiveness and diffusion behavior of sodium lactate loaded chitosan/poly (L-lactic acid) film prepared by coating method as an active packaging.